

A self-assembly template approach for preparing hollow carbon microspheres

Boyang Liu · Dechang Jia · Jiancun Rao ·
Pengjian Zuo · Yingfeng Shao

Received: 15 July 2008 / Revised: 20 October 2008 / Accepted: 22 October 2008 / Published online: 6 November 2008
© Springer-Verlag 2008

Abstract Hollow carbon microspheres (HCMs) are prepared in a sealed quartz tube via the reaction between ferrocene and ammonium bromide. The morphology and microstructure of the product are characterized by X-ray diffraction, Raman spectroscopy, scanning electron microscopy, focused ion beam workstation, transmission electron microscopy, and differential scanning calorimetry analysis. The diameter of the HCMs ranges from 1 to 13 μm and the thickness of shells ranges from 70 nm to 450 nm. It is concluded that the self-generated spherical droplets of iron amine bromide serve as the core templates for the formation of HCMs.

Keywords Hollow carbon microspheres · Ferrocene · Synthesis · Self-assembly · Differential scanning calorimetry

Introduction

The development of portable devices in recent years has underlined the need for small and efficient lithium-ion batteries. In fact, lithium metal is the most attractive anode material in rechargeable batteries because of its large

negative electrode potential and high specific capacity. However, lithium electrode has serious problems because it does not have long enough cycling life and may have safety problems caused by dendrites growing upon cycling [1].

As alternative anode materials, carbonaceous materials are extensively used in lithium-ion batteries due to their low cost, suitable working potential, long cycling life, high cycle efficiency, and safety [2]. Therefore, various carbon types including natural and synthetic graphites, carbon nanotubes, amorphous carbon, cokes and mesocarbon microbeads, etc., have been investigated as the electrodes in lithium-ion batteries [3–6]. However, the high irreversible capacity loss in the first cycle and poor high rate charge/discharge performance, which involves electrolyte decomposition and solid electrolyte interface (SEI) layer formation, are still the problems in carbonaceous anode materials [7]. Fortunately, studies show that the particle size, surface area, electrode thickness, and porosity can have a significant influence on the electrochemical performance of anode materials [8], thus leading to the control preparation of new carbon materials with different structures and forms for practical needs in lithium-ion batteries.

Hollow carbon spheres, with different diameters, hollow interiors, and low density, are attractive in recent years and have several advantages as an anode material [9]. (1) Spherical shapes give a close-packed arrangement, providing a high packing density in cells to allow a high volumetric energy density. (2) The low surface area of hollow carbon microspheres (HCMs) results in less side reactions on the surface during charge and discharge, reducing the irreversible capacity [10]. (3) Hollow carbon spheres of thin shells, which facilitate the transport of lithium ions by offering a shorter solid-state diffusion path, are competent for high charge/discharge rates cells demanded in electric vehicles [11]. (4) Hollow carbon

B. Liu (✉)
Institute of Marine Materials Science and Engineering,
Shanghai Maritime University,
Shanghai 201306, China
e-mail: boyang.liu@yahoo.com.cn

D. Jia · J. Rao · Y. Shao
Institute for Advanced Ceramics, Harbin Institute of Technology,
Harbin 150001, China

P. Zuo
Department of Applied Chemistry, Harbin Institute of Technology,
Harbin 150001, China

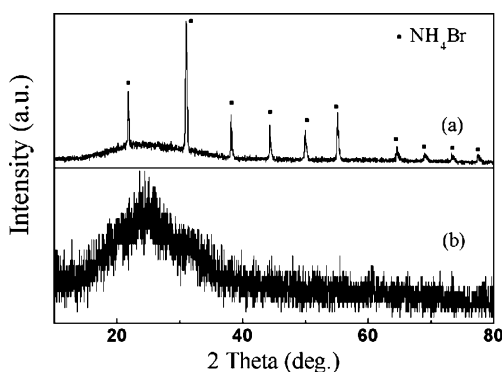


Fig. 1 XRD patterns of **a** the as-prepared product collected in the sealed quartz tube and **b** product after the acid washing process

spheres, serving as protectors, can provide void spaces for other anode materials suffering from great volume change and aggregation problems during charge and discharge [12].

In our previous paper [13], a convenient and efficient method has been suggested for preparation of HCMs with several micrometers in diameter using ferrocene and ammonium chloride as reactants in high pressure argon. The spherical droplets of iron amine chloride are regarded as the self-generated core templates for carbon enwrapping to form HCMs. In this paper, ammonium bromide is used instead of ammonium chloride to synthesize HCMs in a sealed quartz tube because ammonium bromide tends to react with iron to form various iron amine bromides which can also serve as liquid core templates at high temperature like iron amine chloride.

Experimental

In a typical experiment, 100 mg ferrocene and 300 mg ammonium bromide were put into a quartz tube (about 30 ml in volume) which was then sealed after pumping. Next, the tube was heated in an air furnace to 500°C at a ramp rate of $20^\circ\text{C}\cdot\text{min}^{-1}$. After being held for 30 min, the furnace was cooled down naturally. The as-prepared product was collected by breaking the tube, thoroughly washing with HCl solution and deionized water for several times in sequence, and dried in an oven at 100°C for 12 h.

Structure of the product was characterized by X-ray diffraction (XRD, Shimadzu xrd-6000, operated at 30 kV and 40 mA) with $\text{CuK}\alpha$ radiation ($\lambda=1.5418 \text{ \AA}$) and Raman spectroscopy (Labram HR 800, Jobin-Yvon). Morphology of the product after washing was recorded on field emission scanning electron microscopy (MX2600FE, Camscan, 20 kV), focused ion beam workstation (FIB, FEI quanta 200 3D) and transmission electron microscopy (TEM, Philips-CM12, 120 kV). Differential scanning calorimetry (DSC) analysis of the as-prepared powder was conducted on

Netzsch STA 449C at a ramp rate of $10^\circ\text{C}\cdot\text{min}^{-1}$ using a high pressure pan (sealed system) in Ar atmosphere.

Results and discussion

Figure 1a provides the typical XRD pattern of the as-prepared product before acid washing and all the sharp diffraction peaks can be well indexed as NH_4Br (JCPDS 36-1469), suggesting that NH_4Br is excessive in the experiment. In fact, the purpose of adding excess NH_4Br is to prepare HCMs of thin shells, which will be further discussed below. The broad peak around $2\theta=26^\circ$ with low peak intensity corresponds to the HCMs and it becomes evident when the residual NH_4Br and other byproducts are removed by the acid washing process, as shown in Fig. 1b, indicating that the HCMs are amorphous, probably due to the low synthesis temperature.

For further characterizing the structure of the HCMs, the Raman spectrum is recorded at room temperature, as shown in Fig. 2. The prominent peaks at $1,337 \text{ cm}^{-1}$ and $1,590 \text{ cm}^{-1}$ correspond to the carbon D-band and G-band vibration mode, respectively. The G-peak originates from the vibrations of sp^2 -bonded carbon atoms in a two-dimensional graphite plane, while the D-peak is related to double-resonance Raman process in disordered carbon [14]. In principle, the larger the amount of defects, the higher the D-band intensity [15]. Thus, the graphitization of HCMs is low, which is consistent with the XRD pattern (Fig. 1b).

Figure 3a shows the SEM image of the product after washing. It is clearly demonstrated that the majority of the product exhibits spherical morphology and the diameters of the HCMs vary from 1 to $13 \mu\text{m}$, indicating that the yield of the HCMs is high. Unfortunately, lots of HCMs of thin shell and large diameter have low break-down strength and may be destroyed in the washing process owing to the osmotic pressure [16]. The broken HCMs and fragments of the shells strongly prove that the spheres have hollow

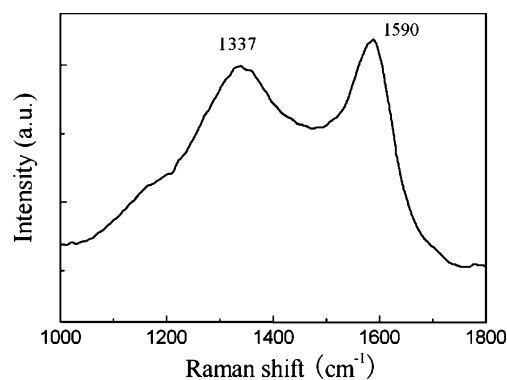


Fig. 2 Raman spectrum of the HCMs

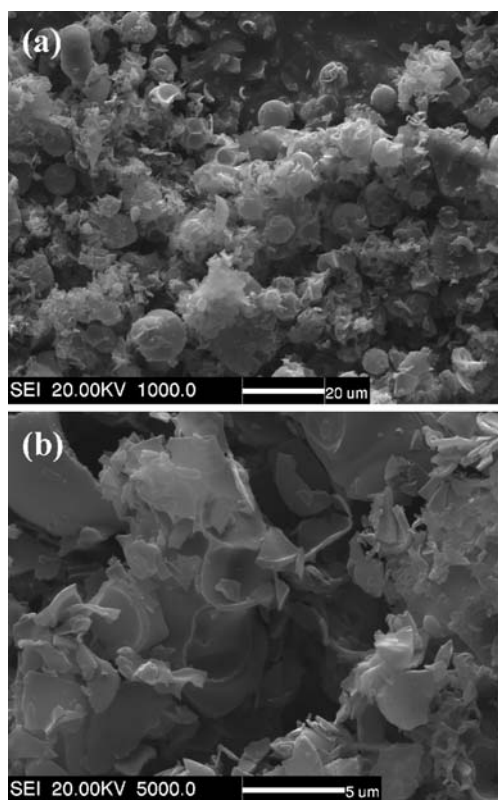


Fig. 3 SEM images of **a** the HCMs and **b** the fragments of the shells

structures. Figure 3b is a high magnification image of the fragments of the shells. It is shown that the thickness of the shells ranges from 70 nm to 450 nm.

In order to prove the large spheres also have hollow structures, FIB workstation, which has the ability to accurately cut a specimen in the scale of micrometers or nanometers at any user-defined position and clearly display corresponding images, is used to in situ cut off the HCMs. Figure 4a shows that the HCMs of large diameters, though some of them are hollow according to the broken ones, of some intact spheres should be further examined. Thus, an intact sphere (in the square region) is chosen for in situ FIB etching. After the in situ experiment has been terminated, it is clearly shown that the large sphere has hollow structure, as shown in Fig. 4b. Moreover, the shell thickness of the hollow sphere of 7 μm in diameter is only about 100 nm.

Figure 5 shows the TEM image of a broken and shrivelled hollow carbon sphere. Though the diameter of the sphere is about 2.5 μm , the hollow structure can be indicated by the pale interior and dark edge even at an acceleration voltage of 120 kV because the thickness of the shell is only about 100 nm. Therefore, it is apparent that HCMs with large diameter and thin shell can be successfully prepared by the reaction of ferrocene and NH_4Br . However, the washing process, which merits further study, should be improved in order to reduce the damage of the HCMs for their practical applications.

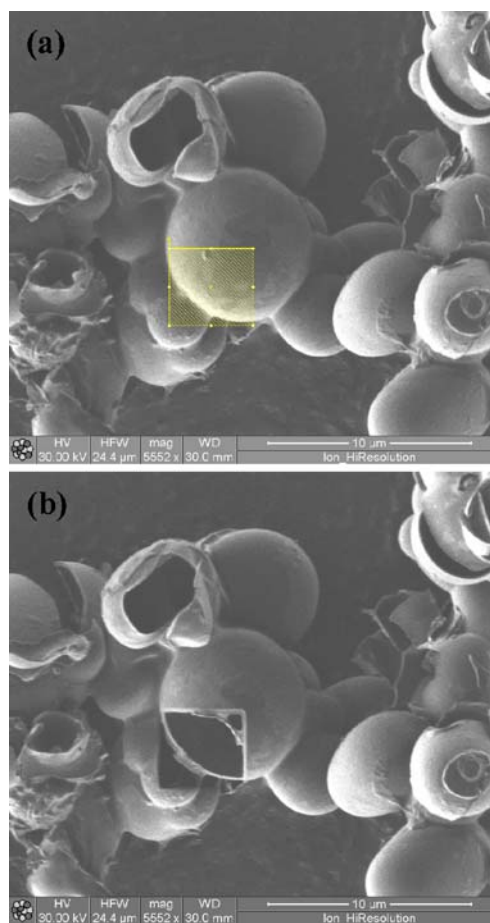


Fig. 4 SEM images of the HCMs **a** before and **b** after the FIB etching

In our previous paper, ferrocene and NH_4Cl are used as reactants to prepare HCMs in a gas pressure furnace. The formation mechanism is proposed as follows [13]: carbon and iron can be formed in advance by the decomposition of ferrocene vapor at about 400 $^\circ\text{C}$ and the nanosized iron

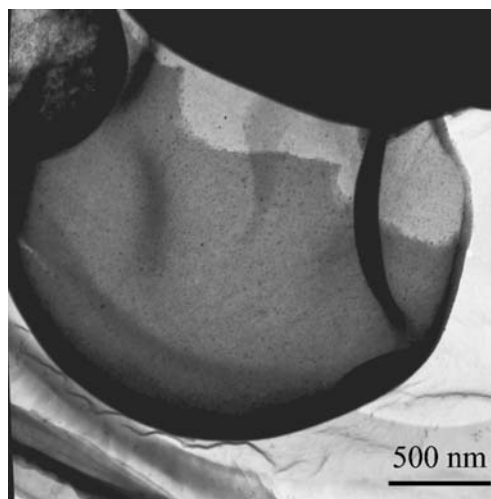


Fig. 5 TEM image of a broken and shrivelled hollow carbon sphere

particles can grow quickly at such a high temperature due to aggregation. As temperature is increased further, iron particles react with NH_4Cl to form iron amine chloride, which are spherical droplets rather than particles as the temperature is higher than its melting point. The droplets serve as the templates, whose surfaces have a relatively higher sticking coefficient and are therefore preferred adsorption sites for the arriving carbon feedstock, resulting in the formation of HCMs.

As we know, NH_4Br also tends to react with iron to form various iron amine bromides [17–19], which may serve as spherical liquid templates for carbon enwrapping at high temperature like iron amine chloride. Although the XRD pattern of the as-prepared product only shows the existence of NH_4Br and HCMs (Fig. 1a), the powder smells of camphor and hydrolyzes in water to produce a green gelatinous precipitate (should be $\text{Fe}(\text{OH})_2$), which are identical with the as-prepared product synthesized by the reaction of ferrocene and NH_4Cl , suggesting the existence of iron amine bromide whose content may be too low to be detected by XRD. However, DSC is suitable for micro-analysis and the measurement of the as-prepared powder is carried out in a sealed pan to prevent the decomposition of the iron amine bromide. The result is similar to that of the earlier work when NH_4Cl is used as the reactant, as shown in Fig. 6. The endothermic peak at 330 °C in the heating curve and the corresponding exothermic peak in the cooling curve at about 330 °C should represent the thermal property of the iron amine bromide considering that HCMs and NH_4Br in the product do not have any reactions or phase transitions in the temperature range. And the two peaks probably represent a physical change and are much like that in melt–freeze transition. The temperature difference between the two peaks should be attributed to the degree of supercooling. Consequently, the iron amine bromide in the as-prepared powder is liquid at high temperature and its melting point is about 330 °C. And during the synthesis of HCMs, after the decomposition of ferrocene above 400 °C,

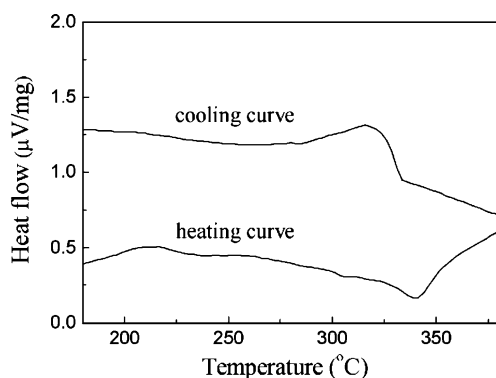


Fig. 6 The DSC curves of the as-prepared powder using a high pressure pan

the generated iron will react with NH_4Br to produce iron amine bromide which should be liquid spheres for the temperature is higher than its melting point. Thus, the formation of HCMs in the experiment is probably caused by the self-generated spherical droplets of the iron amine bromide. Based on the formation mechanism of HCMs, the excess NH_4Br will react with iron particles to reduce their aggregation at high temperature and make the maximum generation of the droplets of iron amine bromide. Thus, there are more adsorption sites for carbon decomposed from ferrocene, leading to the formation of HCMs of thin shells.

Compared with the previous synthesis process conducted in gas pressure furnace, it is found that ferrocene and NH_4Br can also be used to prepare HCMs because iron amine bromide similarly has low melting point and serves as the self-generated liquid core templates for carbon enwrapping. The excess ammonium bromide is helpful for the formation of HCMs of thin shells. Thus, it is concluded that the ammonium halide can be commonly used to prepare HCMs. The extended reactants make the method appropriate for effective synthesis of HCMs. Moreover, in this paper, the experiment is carried out in a sealed vacuum quartz tube, in which the gas pressure is much lower than that in the gas pressure furnace. And it is found that ferrocene and NH_4Cl could also be used to prepare HCMs in a sealed quartz tube (data not shown here). Thus, it is deduced that the sealed reactor is the key factor to prepare HCMs rather than the gas pressure. For iron amine complexes, which are usually prepared in autoclaves, can be maintained without decomposition to serve as templates at high temperature in the sealed reactor. Accordingly, the low synthesis temperature and no special need for the high pressure resist of the equipment will make the large scale preparation of HCMs more attractive in the future and the thin shells are suitable for high rate charge–discharge lithium-ion batteries with optimization of the synthesis process. The method also has certain reference significance to the synthesis of other hollow materials. However, washing process without destroying the HCMs should be further investigated because it is an important prerequisite for the further use of these HCMs. We think that some new techniques may be competent for this purpose such as using different solvents to reduce the surface tension.

Conclusion

HCMs can be prepared via the reaction between ferrocene and ammonium bromide in a sealed quartz tube and the excess ammonium bromide is helpful for the formation of HCMs of thin shells. The diameter of the HCMs ranges from 1 to 13 μm and the thickness of shells ranges from

70 nm to 450 nm. It is concluded that the self-generated spherical droplets of iron amine bromide serve as the core templates for the formation of the HCMs. This method will be attractive for preparation of HCMs for the high rate anode materials in the future.

References

1. Tatsumi K, Iwashita N, Sakaebe H, Shioyama H, Higuchi S (1995) *J Electrochem Soc* 142:716. doi:10.1149/1.2048523
2. Tirado JL, Santamaría R, Ortiz GF, Menéndez R, Lavela P, Jiménez-Mateos JM, Gómez García FJ, Concheso A, Alcántara R (2007) *Carbon* 45:1396. doi:10.1016/j.carbon.2007.03.041
3. Schoonman J (2000) *Solid State Ion* 135:5. doi:10.1016/S0167-2738(00)00324-6
4. Yang ZH, Wu HQ (2001) *Solid State Ion* 143:173. doi:10.1016/S0167-2738(01)00852-9
5. Shi H (1998) *J Power Sources* 75:64. doi:10.1016/S0378-7753(98)00093-7
6. Nishizawa M, Hashitani R, Itoh T, Matsue T, Uchida I (1998) *Electrochem Solid St* 1:10. doi:10.1149/1.1390618
7. Zhang SS, Ding MS, Xu K, Allen J, Jow TR (2001) *Electrochem Solid St* 4:A206. doi:10.1149/1.1414946
8. Zaghba K, Brochua F, Guerfia A, Kinoshita K (2001) *J Power Sources* 103:140. doi:10.1016/S0378-7753(01)00853-9
9. Wang Y, Su FB, Lee JY, Zhao XS (2006) *Chem Mater* 18:1347. doi:10.1021/cm052219o
10. Mabuchi A, Fujimoto H, Tokumitsu K, Kasuh T (1995) *J Electrochem Soc* 142:3049. doi:10.1149/1.2048684
11. Li NC, Mitchell DT, Lee KP, Martina CR (2003) *J Electrochem Soc* 150:A979. doi:10.1149/1.1581259
12. Lee KT, Jung YS, Oh SM (2003) *J Am Chem Soc* 125:5652. doi:10.1021/ja0345524
13. Liu BY, Jia DC, Meng QC, Rao JC (2007) *Carbon* 45:668. doi:10.1016/j.carbon.2006.12.001
14. Shen JM, Li JY, Huang Z, Chen Q, Zhang S, Qian YT (2006) *Carbon* 44:2171. doi:10.1016/j.carbon.2006.03.008
15. Antunes EF, Lobo AO, Corat EJ, Trava-Airoldi VJ, Martin AA, Veríssimo C (2006) *Carbon* 44:2202. doi:10.1016/j.carbon.2006.03.003
16. Yang M, Ma J, Ding SJ, Meng ZK, Liu JG, Zhao T, Mao LQ, Shi Y, Jin XG, Feng YF, Yang ZZ (2006) *Macromol Chem Phys* 207:1633. doi:10.1002/macp.200600273
17. Thiele G, Honert D, Rotter H (1992) *Z Anorg Allg Chem* 616:195. doi:10.1002/zaac.19926161032
18. Eßmann R, Kreiner G, Niemann A, Rechenbach D, Schmieding A, Sichla T (1996) *Z Anorg Allg Chem* 622:1161. doi:10.1002/zaac.19966220709
19. Bremm S, Meyer G (2003) *Z Anorg Allg Chem* 629:1875. doi:10.1002/zaac.200300142